International Journal of Biological Macromolecules 44 (2009) 278–285

Contents lists available at ScienceDirect

International Journal of Biological Macromolecules

journal homepage: www.elsevier.com/locate/ijbiomac

Effects of mobile phone radiofrequency on the structure and function of the normal human hemoglobin

Seyed Jafar Mousavy[a], Gholam Hossein Riazi[a], Mahmood Kamarei[b], Hadi Aliakbarian[b], Naghmeh Sattarahmady[a,f], Ahmad Sharifizadeh[a], Shahrokh Safarian[c], Faizan Ahmad[d], Ali Akbar Moosavi–Movahedi[a,e,*]

[a] Institute of Biochemistry and Biophysics, University of Tehran, Tehran, Iran
[b] Faculty of Electrical and Computer Engineering, University of Tehran, Tehran, Iran
[c] School of Biology, College of Science, University of Tehran, Tehran, Iran
[d] Centre for Interdisciplinary Research in Basic Sciences, Jamia Millia Islamia, Jamia Nagar, New Delhi, India
[e] Foundation for Advancement of Science and Technology in Iran (FAST-IR), Tehran, Iran
[f] Department of Biochemistry, Shiraz University of Medical Sciences, Shiraz, Iran

ARTICLE INFO

Article history:
Received 14 December 2008
Received in revised form 5 January 2009
Accepted 6 January 2009
Available online 15 January 2009

Keywords:
Mobile phone radiofrequency
Hemoglobin
Conformational changes
Oxygen affinity

ABSTRACT

Widespread use of mobile phones has increased the human exposure to electromagnetic fields (EMFs). It is required to investigate the effect of EMFs on the biological systems. In this paper the effect of mobile phone RF (910 MHz and 940 MHz) on structure and function of HbA was investigated. Oxygen affinity was measured by sodium dithionite with UV–vis spectrophotometer. Structural changes were studied by circular dichroism and fluorescence spectroscopy. The results indicated that mobile phone EMFs altered oxygen affinity and tertiary structure of HbA. Furthermore, the decrease of oxygen affinity of HbA corresponded to the EMFs intensity and time of exposure.

1. Introduction

Nowadays, more than 2.5 billion people utilize cell phones and base stations constituting the cell network. The global system for mobile communication (GSM) which being used in most of the countries has a frequency of either 900 or 1800 MHz (pulsed at 217 Hz, band width of 200 kHz). The spectrum of 900 MHz has two bands: 890–915 MHz which is specific for handset, and 935–960 MHz which is specific for base station antenna. The development of mobile communication has aroused a deep interest in people and has stimulated wide and often controversial discussions in the scientific community about potential damages induced by exposure to low-level radiation emitted in the microwave (MW) region [1].

There are several works on the effect of electromagnetic fields (EMFs) on proteins. The possibility that RF radiation may cause changes in protein conformation and hence biological properties has been reported in Refs. [2–9]. George et al. [10] studied citrate synthase unfolding by the effect of EMFS, and concluded that microwaves have effect on protein conformation that could take the form of a direct interaction of the electromagnetic fields with the protein or its water of hydration. In another work Mancinelli et al. [11] also showed the same result, exploring a potential role of MW-EMFs exposure in affecting folding process and/or determining the misfolding of polypeptide chains. Exposure to cell phone radiation up-regulates apoptosis of genes in primary cultures of neurons and astrocytes [12], and in human endothelial cell lines [13]. Also expression of Hsp70 [14,15]; early gene, c-fos [16]; G1 phase-regulating proteins [17]; tumor suppressor p53 [18]; up-regulating P27Kip1 [19] affected by microwave irradiation.

It has reported the change in the activity of enzymes upon exposure by microwave EMFs, e.g., extracellular-signal-regulated kinase [20]; antioxidative enzyme activities [21]; trichoderma reesei cellulase [22]; Na, K-ATPase [23]; acetylcholinesterase [24,25]; soluble and insoluble peroxidase [26]; cerebral cytochrome *c* oxidase [27].

Schirmacher et al. [28] reported the influence of high frequency EMFs on the permeability of an in vitro model of the blood–brain barrier (BBB). They concluded that on exposure to EMFs the permeability of ^{14}C-sucrose increased significantly compared to that of the unexposed samples.

In light of what happen to biological systems by exposing to the EMFs, there are some evidences for possible effects of EMF via involving in electron transfer reactions. These were extensively

* Corresponding author at: Institute of Biochemistry and Biophysics, University of Tehran, Tehran, Iran. Tel.: +98 21 66403957; fax: +98 21 66404680.
E-mail address: moosavi@ibb.ut.ac.ir (A.A. Moosavi–Movahedi).

0141-8130/$ – see front matter © 2009 Elsevier B.V. All rights reserved.
doi:10.1016/j.ijbiomac.2009.01.001

reported by Blank and coworkers [9,23,29–39]. Blank and Soo [34] were also examined the EM field effects on electron transfer by using simple system, the classic oscillating Belousov-Zhabotinski (BZ) reaction. They concluded that EM fields accelerate all linked redox reactions. In other work [39] they concluded that 60 Hz magnetic fields accelerate electron transport from cytochrome *c* to the enzyme, cytochrome oxidase. In other studies, they demonstrated the effects of low frequency electric and magnetic fields on several biochemical systems, including the Na,K-ATPase, and indicate that EMFs interact with electrons [23,33]. In recent review paper, Blank [9] was considered examples of direct effects of electric and magnetic fields on charge transfer in biological systems, and reported the structural changes driven by such effects. Blank [9] also concluded that conformational changes that arise from alterations in charge distribution play a key role in membrane transport proteins, including ion channels, and probably account for DNA stimulation to initiate protein synthesis. In conclusion it appears likely that weak EMFs can control and amplify biological processes through their effects on charge distribution.

Behind these works there are also several papers showed that the EMFs had no effects on biological systems. Schwarz et al. [40] reported the genotoxic effects of Radiofrequency EMFs (GSM, 1950 MHz) in vitro in human fibroblasts but not in lymphocytes. They concluded that GSM exposure may cause genetic alterations in some but not in all human cells in vitro. Martino et al. [41] showed that pulsed EMFs did not affect on the metabolic activity and cell number of SaOS-2 osteoblast-like cells. Mobile phone exposure does not induce apoptosis on spermatogenesis in rats which were reported by Dasdag et al. [42]. Stefanics et al. [43] reported a single 10 min exposure of 900 MHz EMFs emitted by a commercial mobile phone does not produce measurable immediate effects in the latency of auditory brainstem waves I, III and V. Leadbeater et al. [44] showed that microwave irradiation on the lipase-catalysed transesterification reaction of methyl acetoacetate does not have a noticeable effect on reaction rate or product conversion. Mobile phone base station-emitted radiation does not induce phosphorylation of Hsp27 reported by Hirose et al. [45]. Ferreira et al. [46] showed that high frequency EMFs exposure on the central nervous system of rats is not able to produce detectable oxidative stress. Zeng et al. [47] reported that RF EMFs exposure under experimental conditions cannot produce distinct effects on gene and protein expression in the MCF-7 cells. Thorlin et al. [48] suggested that exposure of cultured astroglial and microglial brain cells to 900 MHz microwave radiation does not provide evidence for any effect. Bismuto et al. [1] showed that Measurements of absorption spectroscopy, circular dichroism and fluorescence emission decay in the frequency domain do not exhibit any influence of the microwave radiation on the native structural state of myoglobin. Li et al. [49] reported that 837 MHz microwave exposure of TP53 tumor suppressor protein in normal human fibroblasts do not change significantly.

Normal hemoglobin (HbA) is an essential component of the circulatory system of vertebrates. Its chief physiological function is to transport oxygen from the lungs to the tissues [50]. Hemoglobin (molecular weight 64,500) is roughly spherical, with a diameter of nearly 5.5 nm. It is a tetrameric protein containing four heme prosthetic groups, each one associated with each polypeptide chain. Adult hemoglobin contains two types of globin, two α chains (141 residues each) and two β chains (146 residues each). Although, fewer than half of the amino acid residues in the polypeptide sequences of α- and β-globins subunits are identical, the three-dimensional structures of the two types of subunits are very similar.

In arterial blood passing from the lungs through the heart to the peripheral tissues, hemoglobin is about 96% saturated with oxygen [51,52]. In the venous blood returning to the heart, hemoglobin is only about 64% saturated [52]. Hemoglobin, with its multiple subunits and O_2-binding sites, is better suited to oxygen transport. Interactions among the subunits in hemoglobin caused conformational changes that alter the affinity of the protein for oxygen [53,54]. The modulation of oxygen binding allows the O_2-transport protein to respond to changes in oxygen demand by tissues. Hemoglobin must bind oxygen efficiently in the lungs, where the pO_2 is about 13.3 kPa, and release oxygen in the tissues, where the pO_2 is about 4 kPa. Myoglobin, or any protein that binds oxygen, and this binding is described by a hyperbolic binding curve, would be ill suited to this function. A protein that binds O_2 with high affinity would bind it efficiently in the lungs but would not release much of it in the tissues. If the protein that binds oxygen with a sufficiently low affinity to release it in the tissues, it would not pick up much oxygen in the lungs. Hemoglobin solves the problem by undergoing a transition from a low-affinity state (the T state) to a high-affinity state (the R state) as more O_2 molecules are bound. As a result, hemoglobin has a hybrid S-shaped, or sigmoid, binding curve for oxygen [55].

In addition to carrying nearly all the oxygen required by cells from the lungs to the tissues, hemoglobin carries two end products of cellular respiration (H^+ and CO_2) from the tissues to the lungs and the kidneys, where they are excreted. Carbon dioxide must be hydrated and therefore results an increase in the H^+ concentration (a decrease in pH) in the tissues. The binding of oxygen by hemoglobin is profoundly influenced by pH and CO_2 concentration, so the interconversion of CO_2 and bicarbonate is of a great importance to the regulation of oxygen binding and release in the blood. Hemoglobin transports about 40% of the total H^+ and 15–20% of the CO_2 formed in the tissues to the lungs and the kidneys. The binding of H^+ and CO_2 is inversely related to the binding of oxygen. At the relatively low pH and high CO_2 concentration of peripheral tissues, the affinity of hemoglobin for oxygen decreases as H^+ and CO_2 are bound, and O_2 is released to the tissues. Conversely, in the capillaries of the lung, as CO_2 is excreted and the blood pH consequently rises, the affinity of hemoglobin for oxygen increases and the protein binds more O_2 for transport to the peripheral tissues. This effect of pH and CO_2 concentration on the binding and release of oxygen by hemoglobin is called the Bohr effect, after Christian Bohr, the Danish physiologist who discovered it in 1904. The O_2–saturation curve of hemoglobin is influenced by the H^+ concentration. Both O_2 and H^+ are bound by hemoglobin, but with inverse affinity. When the oxygen concentration is high, as in the lungs, hemoglobin binds O_2 and releases protons. When the oxygen concentration is low, as in the peripheral tissues, H^+ is bound and O_2 is released. Oxygen and H^+ are not bound at the same sites in hemoglobin. Oxygen binds to the iron atoms of the hemes, whereas H^+ binds to any of several amino acid residues in the protein [51,55–58].

2,3-disphosphoglycerate (DPG) is another molecule which contribute in hemoglobin function. DPG is known to greatly reduce the affinity of hemoglobin for oxygen. There is an inverse relationship between the binding of O_2 and the binding of DPG and binds at a site distant from the oxygen-binding site and regulates the O_2-binding affinity of hemoglobin in relation to the pO_2 in the lungs [55,59].

In this research we attempted to study the effect of mobile phone EMFs on the oxygen affinity and structure of HbA, because of the importance of hemoglobin as a sole oxygen transporter in blood.

2. Materials and methods

2.1. Materials

All chemicals were purchased from Merck (Germany). These were of analytical grade and were used without further purification.

All measurements were made in triplicate at 37.0 ± 0.1 °C unless otherwise indicated.

2.2. Methods

2.2.1. Preparation of hemoglobin

Human adult hemoglobin (HbA) was prepared from human red blood cells of healthy donors. The heparinized blood was centrifuged to remove plasma components. The packed red cells were washed three times in an isotonic saline solution (0.9% NaCl) and red cells were osmetically lysed with cold double distilled water. Membrane components were removed by low-speed centrifugation (3000 rpm). The soluble Hb was centrifuged at least two additional times at high speed to remove any insoluble materials (10,000 rpm). The hemoglobin solution was then brought to 20% saturation with ammonium sulfate, left standing for about 15 min, and centrifuged at 20,000 × *g* for 1 h at 2 °C. The supernatant contained HbA [60].

2,3-diphosphoglycerate was removed by method of Benesch et al. [61]. HbA samples were dialyzed at least three times in 50 mM phosphate buffer (pH 7.5) for 24 h. The hemoglobin concentration was determined spectrophotometrically using a millimolar extinction coefficient of 13.5 (monomer basis) at 541 nm for oxyhemoglobin [62]. Additionally, the samples were analyzed by conventional sodium dodecyl sulfate polyacrylamide gel electrophoresis (SDS-PAGE) for purity.

2.2.2. Exposure setup

Exposure of HbA to the RF 910 MHz and 940 MHz EMF were carried by a spiral antenna (frequency range: 800 MHz to 12 GHz) in a temperature controlled incubator in the shielded room of the Antenna Laboratory of the University of Tehran (see Fig. 1).

If the sample is situated far from the antenna, it can be assumed that the incident signal is a plane wave. The electric field intensity (EFI) in the location of the sample has been measured using an E-field probe and a calibrated spectrum analyzer at 37.0 ± 0.1 °C.

RF continuous wave without any modulation is generated by the HP 8657A signal generator. As the output power level of the signal generator is limited to 15 dBm (decibel referenced to mW), a high power WicomTech GSM amplifier is added to guarantee the power requirements.

The HbA sample (3 mL of solution) in a polystyrene tube was exposed to the 910 MHz or 940 MHz EMF. Temperature was controlled to within ± 0.1 °C by the incubator manufactured by PERSSOJEN CO (Iran). The treated sample was matched with unexposed control which was kept in the same experimental conditions, except this was isolated in a 10-mm thickness aluminum sample holder with an aluminum cap.

The cable carries the signal from the E-field probe to the spectrum analyzer, which has 2.5 dBm losses. Observed power by the spectrum analyzer (e.g., 21 dBm) shows that power on the sample is equal to 23.5 dBm or 233.87 mW. Assuming the dipole antenna (probe) has a resistance, with $R = 50\ \Omega$ and length, $L = 6.1$ cm, the electric field intensity of 37.7 dBV/m or 77 V/m was determined on the sample, which is equal to 2 dBm/cm^2 or 15.7 W/m^2 using the relation:

$$U = \frac{E^2}{\eta} \text{ Or } U_{dB} = 2E_{dB} - 25.7_{dB} \quad (1)$$

where E is the electric field intensity (EFI), η is the free space characteristic impedance (377 Ω), and U is the power density.

The hemoglobin sample is holded inside the plastic tube with 5 cm in length and 1 cm in diameter. The change of temperature inside the tube upon interaction with mobile phone radiation is calculated and it was negligible.

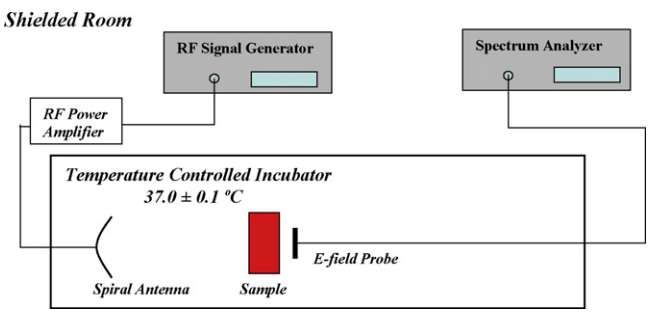

Fig. 1. A block diagram for exposing the HbA samples.

2.2.3. Measurements of the oxygen affinity of HbA

Oxygen affinity of hemoglobin was measured on the basis of differences in spectral characteristics between the two pigments, oxyhemoglobin and deoxyhemoglobin as described by Tietz [63]. Absorbance of 800 μL HbA in 10 mM phosphate buffer (pH 7.4) was determined at 548 and 577 nm. These were designated $A_{548(o)}$ and $A_{577(o)}$, respectively, where subscript o represents oxygenated protein. 100 μL of sodium dithionite ($Na_2S_2O_4$) solution [3 mg/mL] was added to these oxygenated solutions, mixed gently, and then absorbance was measured at 548 and 577 nm. Which are designated as $A_{548(r)}$ and $A_{577(r)}$, respectively, where the subscript r represents the deoxygenated HbA. Ratio of R_o and R_r as well as constants K_4 and K_5 were calculated as follows [63]:

$$R_o = \frac{A_{548(o)}}{A_{577(o)}} \quad (2)$$

$$R_r = \frac{A_{548(r)}}{A_{577(r)}} \quad (3)$$

$$K_4 = \frac{100}{(R_o - R_r)} \quad (4)$$

$$K_5 = \frac{100\,R_r}{(R_o - R_r)} \quad (5)$$

The fresh HbA solution (800 μL) was placed into the cell of spectrophotometer and absorbance at 548 and 577 nm was read. This solution was titrated with several addition of 5 μL solution of sodium dithionite. During each addition, solution was mixed gently and absorbance was measured at 548 and 577 nm after 3 min. The titration was carried out till all oxygen was removed from HbA. Percent saturation of HbA with O_2 for each step was calculated as follows:

$$\text{Percent saturation} = K_4 \left(\frac{A_{577}}{A_{548}}\right) - K_5 \quad (6)$$

Molar concentration of sodium dithionite [SDT], required for 50% saturation of HbA, is designated as $[SDT]_{50}$. This is practically equivalent to P_{50} in oxygen dissociation curve of Hb [55]. The absorbance was recorded in Shimadzu model UV-3100 spectrophotometer whose temperature was maintained at 37.0 ± 0.1 °C by circulating water from an external Haak D8 water bath. All samples were kept in an air-shielded cuvette.

2.2.4. Circular dichroism spectropolarimetry

Circular dichroism (CD) spectra in the far-UV regions (190–260 nm) were obtained in J-810 Jasco spectropolarimeter using 1 mm path cell at 25 °C. Protein concentration (monomer basis) was 21 μM (0.2 mg/mL) in the presence of 10 mM sodium phosphate buffer, pH 7.4. Protein secondary structure was determined by CDNN program, version 2.1.0.223. The visible-CD (350–600 nm) was measured in an Aviv 215 spectropolarimeter at 25 °C. The CD measurement was performed using a 10-mm path length quartz cuvette and a protein concentration of 11 μM.

2.2.5. Fluorescence measurements

A Cary Eclipse Varian Australia spectrofluorescence that was equipped with a temperature controller bath model Cary was used

for the intrinsic fluorescence experiments. The excitation wavelength was adjusted to 285 nm, which was specific for the excitation of tryptophan (Trp) residues of the protein structure. Emission spectra were recorded between the wavelengths of 290 and 400 nm at the bandwidth of 10 nm. Hemoglobin samples were 10.3 μM (monomer basis) in a phosphate buffer (10 mM, pH 7.4).

1-anilinonaphthalene-8-sulfonate (ANS) is a small organic compound that be used to probe for the accessibility of hydrophobic patches in proteins. In this study, protein solution (10.3 μM, monomer basis) was prepared in 1 ml of phosphate buffer (10 mM, pH 7.4) with 10 μL of ANS (2 mM). Emission scans were then obtained from 365 to 600 nm using an excitation wavelength of 355 nm.

2.2.6. Aggregation assays

Time courses of thermal aggregation of HbA solutions (11.3 μM, monomer basis) were followed by measuring absorbance at 360 nm in Cary-100 Bio VARIAN spectrophotometer using a 10-mm path length quartz cuvette [64]. Temperatures were controlled within ±0.1 °C by a Cary temperature controller. Aggregation was followed for 300 min at 60 °C. It is important to note exposed and unexposed hemoglobin samples were in solution at 37 °C and not aggregated.

2.2.7. Thermal denaturation measurements

Thermal denaturation of HbA solutions (10.4 μM, monomer basis) was followed at 280 nm in a Cary-100 Bio VARIAN spectrophotometer using a 10-mm path length quartz cuvette [64]. Temperatures were controlled to within ±0.1 °C by a Cary temperature controller. Absorbance at 280 nm was obtained in temperature range 25–85 °C with a scan rate of 0.5 °C/min. This scan rate was found to provide adequate time for equilibration.

Thermal unfolding of HbA solutions (10.4 μM, monomer basis) was also monitored in J-810 Jasco spectropolarimeter using 2 mm path cell by measuring the decrease in ellipticity at 222 nm with increasing temperature. The dynode voltage changes that occurred with changes in temperature were also recorded and were used as a criterion of protein aggregation [65,66]. Circular dichroism and dynode voltage at 222 nm was obtained in temperature range 25–85 °C with a scan rate of 0.5 °C/min.

3. Results and discussion

3.1. Oxygen affinity

More than 1000 variants of Hb have been reported, some with altered oxygen affinity, either higher or lower while maintaining the stability of Hb. Individuals with low oxygen affinity hemoglobin show mild anemia, whereas individuals with high oxygen affinity hemoglobin shows symptoms associated with polycythemia [67].

Sodium dithionite ($Na_2S_2O_4$) is a powerful reducing agent used to deoxygenate hemoglobin, and it is extensively used for this purpose [68–74]. The reaction takes place between one molecule of dithionite and one of oxygen, with the production of H_2O_2:

$$Na_2S_2O_4 + O_2 + 2H_2O \leftrightarrows 2NaHSO_3 + H_2O_2 \quad (7)$$

We have used this reagent for deoxygenating of HbA.

Fig. 2 shows the percent saturation of HbA in 10 mM phosphate buffer (pH 7.4) in the absence and presence of 940 MHz with an EFI of 77 V/m as a function of [SDT]. We have analyzed each curve using a non-linear least-squares method of $[SDT]_{50}$, the molar concentration of SDT at which HbA is 50% saturated with O_2. These values of $[SDT]_{50}$ were used to determine α, defined as

$$\alpha = 100([SDT]_{50}\text{unexposed} - [SDT]_{50}\text{exposed})/[SDT]_{50}\text{unexposed} \quad (8)$$

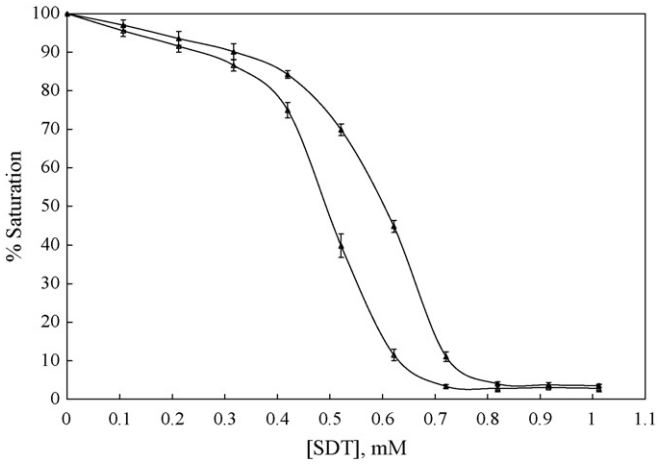

Fig. 2. Effect of 940 MHz with EFI of 77 V/m on HbA. Protein in 10 mM phosphate buffer exposed (△), and unexposed (▲). Experimental conditions: [HbA] = 32.5 μM, exposure time = 1 h and pH 7.4. The effect of 910 MHz is resembled to 940 MHz, data not shown. The error bars indicate of triplicate repeating experiments.

We have also determined α value of HbA in the absence and presence of 940 MHz with EFI of 21.7, 30.6, 48.6 at 10 mM phosphate buffer from the measurements such as shown in Fig. 2 (this figure is plotted for 77 V/m as a typical, other electric field intensity are resemble to Fig. 2). These values are tabulated in Table 1. It is seen in this table that dependence of α on EMFs is not linear; suggesting that α of HbA depends on factor(s) as well. It worth noting that Tkalec et al. [75] suggest the effects of radio frequency fields are frequency dependent and are not linear over the whole field intensity spectrum. Furthermore, several workers have also reported the nonlinearity responses of biological systems to radiofrequency exposure [76–81].

Results presented and discussed above led us to conclude that the O_2 binding ability of HbA is affect by the EMFs intensity. We wanted to know whether the duration to which HbA is exposed to particular EMFs is also important. We have therefore designed experiments in which HbA is exposed to 940 MHz with EFI of 77 V/m (about 1.6 mW/cm^2) for five fixed times (15, 30, 60, 90 and 120 min) and measured % saturation as a function of [SDT]. These results were analyzed for α value for different times of exposure, and are shown in Fig. 3. It is seen in this figure that α increase with an increase in time of exposure. Then exposure of HbA with electric field intensity for long time has more effect on the retardation of the O_2-binding ability of the time.

All the O_2-binding results suggested that EMFs has its effect on the binding ability of HbA. We wanted to know whether there is any relation between this decreased binding ability of HbA and structure of the protein. In order to understand this we carried out structural studies using UV/vis, CD and fluorescence measurements. It should be noted that all structural studies were carried out at 940 MHz with electric field intensity of 77 V/m.

Table 1
Values of α (see Eq. (8)) of HbA in 10 mM phosphate buffer (pH 7.4). The protein was exposed to 940 MHz with different electric field intensities (EFI) at 37 °C. The protein concentration was 32 μM.

$\alpha \pm$ S.D.[a]	EFI (V/m)
−2.20 ± 0.70	21.7
13.46 ± 3.58	30.6
16.46 ± 5.54	48.6
17.01 ± 2.45	77.0

[a] Standard deviation.

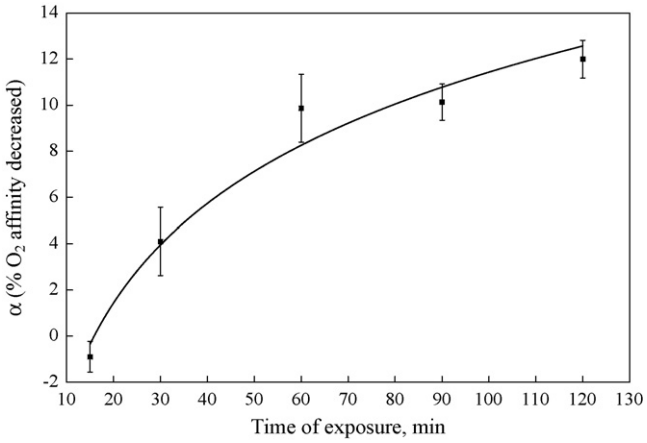

Fig. 3. Time-dependence of the effect of 940 MHz with EFI of 77 V/m on HbA. Experimental conditions: [HbA] = 32 μM in 10 mM phosphate buffer, pH 7.4, at 37 °C. The error bars indicate of triplicate repeating experiments.

3.2. Circular dichroism studies

Fig. 4 shows the far-UV CD spectra of unexposed and exposed HbA in 10 mM sodium phosphate buffer with 940 MHz and EFI of 77 V/m. It is seen in this figure that the exposed protein has slightly more secondary structure. This finding seems to suggest that the secondary structure has no significant role to play in the altered binding ability of HbA under these experimental conditions.

Fig. 5 shows CD spectra of HbA in the Soret band region under same experimental conditions used to obtain results shown in Fig. 4. It may be seen in this figure that globin–heme interaction is affected by an exposure to the radiation. The Soret CD spectra of HbA, which results from the π–π* transition of the heme chromophore, and this transition is influenced by the surrounding aromatic amino acids. Therefore, the Soret CD spectral changes can reflect the changes not only in the electronic state of the heme but also in its environment [82,83]. Visible circular dichroism spectra of the HbA exposed to 940 MHz with EFI of 77 V/m is shown in Fig. 5. The spectral difference in the Soret region indicates that tertiary structure of the protein is significantly changed on the exposure of HbA to EMFs.

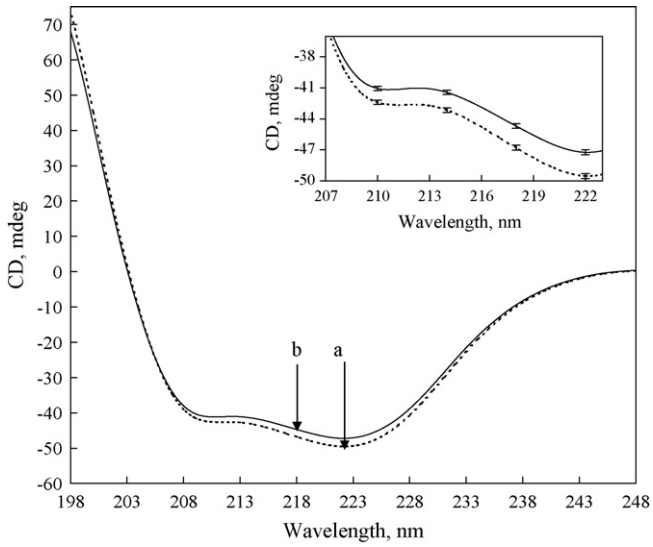

Fig. 4. The far-UV CD spectra of the HbA in 10 mM phosphate buffer (pH 7.4). CD spectra of the exposed (a) and unexposed (b) HbA at 940 MHz with EFI of 77 V/m for 1 h. The HbA concentration was 21 μM. The inset shows error bars of spectra for triplicate repeating experiments and high reproducibility of measurements.

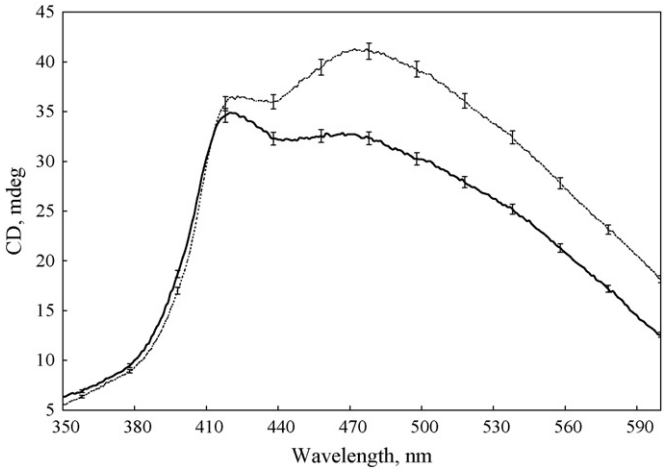

Fig. 5. The visible CD spectra of the HbA at 37 °C. CD spectra of the exposed (a) and unexposed (b) HbA at 940 MHz, 77 V/m for 1 h. The HbA concentration was 11 μM dissolved in 10 mM phosphate buffer at pH 7.4. The error bars of spectra indicate triplicate of repeating experiments and high reproducibility of measurements.

This finding is possibly due to a difference in the tightness of the heme attachment [84], leading to a change in the binding ability of the protein on exposure to the electric field.

3.3. Fluorescence measurements

The Hb molecule is assembled from two symmetrical (αβ) dimmers. Each (αβ) dimmer contains three tryptophan (Trp) residues, adding to a total of six Trp residues in the tetramer. Fluorescence of hemoglobin tetramer is mainly due to the six tryptophan residues [85].

Fig. 6 shows fluorescence spectrum of HbA solution in 10 mM phosphate buffer exposed to 940 MHz with EFI of 77 V/m and compare it with that of the unexposed HbA. This figure shows a quenching of Trp fluorescence with 4 nm blue shift. It is known that a shift of maximum emission wavelength corresponds to a polarity change around the chromophore residues. A red shift always indicates that Trp residues are, on average, more exposed to the solvent and these is a decrease in the fluorescence intensity. On the other hand, a blue shift is a consequence of transferring Trp residues into a more hydrophobic environment and there is an increase in the

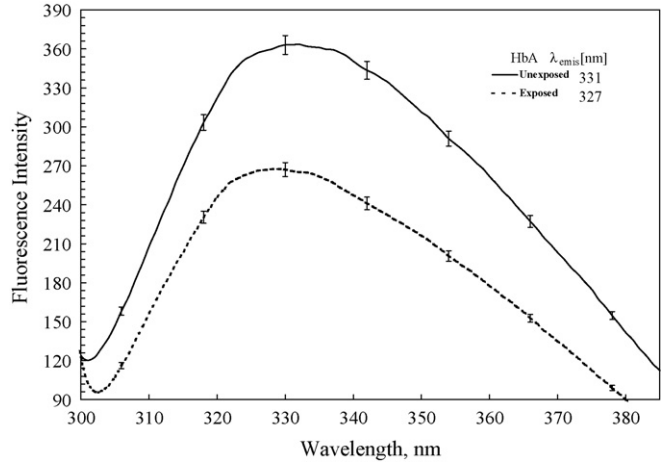

Fig. 6. Fluorescence spectra of HbA in 10 mM phosphate buffer (pH 7.4) at 37 °C. Unexposed (—) and exposed (- - -) proteins. Experimental conditions: [HbA] = 10.2 μM, 940 MHz of EFI = 77 V/m, and exposure time = 1 h. The error bars of spectra indicate of triplicate repeating experiments and high reproducibility of measurements.

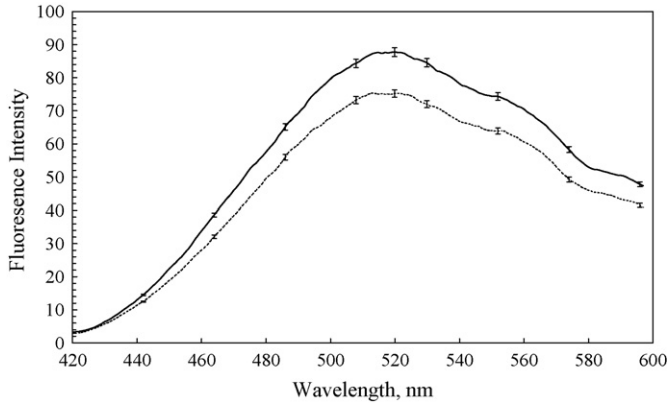

Fig. 7. Fluorescence spectra of ANS binding with exposed (- - -) and unexposed (—) HbA (excitation wavelength was 355 nm). The HbA concentration was 10.3 μM dissolved in 10 mM phosphate buffer (pH 7.4). The protein was exposed with 940 MHz, EFI of 77 V/m for 1 h at 37 °C. The error bars of spectra indicate of triplicate repeating experiments and high reproducibility of measurements.

fluorescence intensity. However, it is observed that although there is a blue shift indicating that Trp is transferred to a more hydrophobic environment, yet fluorescence intensity is decreased (see Fig. 6). This could be due to quenching of the Trp fluorescence by the heme. Our results do suggest that the tertiary structure of the protein is altered on exposure to the EMFs.

The fluorescence probe ANS has often been used for research on biosystems. ANS exhibits a large fluorescence enhancement on binding to the exposed hydrophobic patches of proteins [85]. Fluorescence of ANS in exposed HbA is less than unexposed HbA (see Fig. 7). This finding suggests that the untreated HbA has more hydrophobic patches exposed to solvent than the EMFs exposed protein. Thus, the exposure of HbA to EMFs leads to a more compact structure of the protein.

3.4. Aggregation measurements

Fig. 8 shows the change in A_{360} (a probe for measuring aggregation) of HbA in 10 mM phosphate buffer solution exposed to 940 MHz with EFI of 77 V/m as a function of time at 60 °C. It is seen in this figure that aggregation process of the exposed and unexposed of HbA is similar until 175 min. After that, aggregation of the exposed HbA reached a plateau, but aggregation process of unexposed HbA continued. So, it could be concluded that the extent of aggregation of the exposed HbA is smaller than normal condition. This could be due to the less exposed hydrophobic surface on the protein exposed to the radiation. This observation is in agreement with the intrinsic and ANS fluorescence measurements (see Figs. 6 and 7).

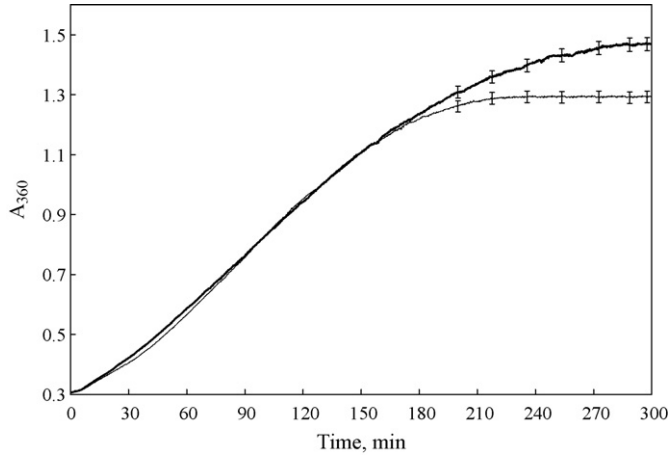

Fig. 8. Time courses for aggregation of HbA in 10 mM phosphate buffer (pH 7.4) at 60 °C. Exposed (a) and unexposed (b) protein. Protein (11.3 μM) was exposed to radiation (940 MHz, EFI = 77 V/m and exposure time = 1 h, at 37 °C) and measurements of absorbance at 360 nm was carried out at 60 °C. The error bars indicate triplicate repeating experiments and high reproducibility of measurements.

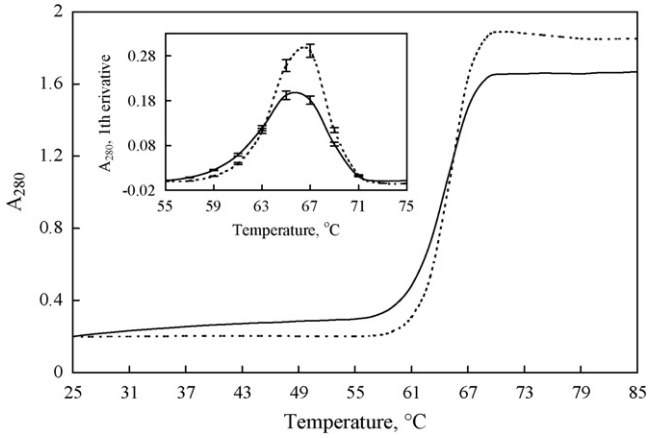

Fig. 9. Heat-induced denaturation of the exposed (- - -) and unexposed (—) HbA in 10 mM phosphate buffer (pH 7.4). Experimental conditions: [HbA] = 10.4 μM, 940 MHz, EFI = 77 V/m, exposure time = 1 h and at 37 °C. Denaturation was monitored by change in absorbance at 280 nm with a heating rate of 0.5 °C/min. The inset shows first derivative of plots of A_{280} vs. temperature. The error bars were showed in the inset indicates of triplicate repeating experiments and high reproducibility of measurements.

3.5. Thermal profiles

Fig. 9 shows thermal denaturation profiles of HbA in 10 mM phosphate buffer unexposed and exposed to 940 MHz with electric field intensity of 77 V/m. This figure indicated the thermal profiles induced by tertiary structure which obtained by UV spectrometer at 280 nm. The inset shows the first derivative of each curve. The maximum in this profile occurs at T_m [86]. It has been observed that the exposed HbA shows 2 °C increasing in T_m suggesting that the exposed HbA structure is slightly more thermal stability relative to the unexposed protein. This finding is also consistent with the fluorescence measurements.

It should be noted that each curve shown in this figure (see Fig. 9) describes at least two phenomena, namely denaturation and aggregation. We wanted to know which of these phenomena are affected by EMFs that exerted in our experiments. Thus, we need to discriminate these two different phenomena (unfolding and aggregation). For this reason we carried out another experiment based on the method used by Benjwal et al. [65]. This method is carried out by circular dichroism (CD) experiments and then used CD data along with dynode voltage data to discriminate between the heat-induced protein unfolding and aggregation. To discriminate these two phenomena we also used this technique.

Fig. 10 shows thermal unfolding and aggregation profiles of HbA in 10 mM phosphate buffer unexposed and exposed to 940 MHz with electric field intensity of 77 V/m used Far-UV circular dichroism spectropolarimetry (accordance to secondary structure of protein). Fig. 10a represents unfolding process and show that onset of unfolding of unexposed protein is resembled with the exposed sample. The figure also indicates that the whole thermal unfolding profile of exposed protein is postponed relative to unexposed sample. Fig. 10b represents aggregation process of HbA that is obtained by dynode voltage at 222 nm as a criterion of aggregation profile. It has been observed in this figure that onset of aggregation

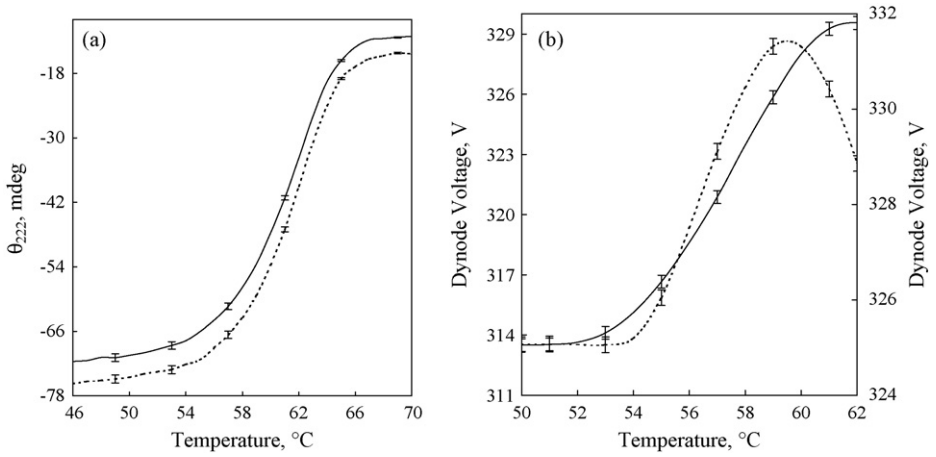

Fig. 10. Thermal unfolding and aggregation of the exposed (- - -) and unexposed (—) HbA in 10 mM phosphate buffer (pH 7.4) monitored by CD and turbidity. (a) CD melting curves, θ_{222} (T), recorded at 222 nm report on a-helical unfolding. (b) Turbidity (dynode voltage) melting curves, V (T), recorded at 222 nm report on the heat-induced increase in the particle size due to protein aggregation. Experimental conditions: [HbA] = 10.4 μM, 940 MHz, EFI = 77 V/m, exposure time = 1 h and at 37 °C. Circular dichroism and dynode voltage at 222 nm was obtained in temperature range 25–85 °C with a scan rate of 0.5 °C/min. The error bars indicate triplicate repeating experiments and high reproducibility of measurements.

of unexposed HbA is about 52 °C but those of exposed protein is at 54 °C. This difference indicates that the structure of the exposed HbA is slightly late aggregate and therefore is more thermal stable relative to the unexposed protein.

The results from Figs. 9 and 10 indicate the thermal conformational change for hemoglobin started near 60 and 55 °C for tertiary and secondary structures, respectively and not any conformational change occurred at near 37 °C for exposed and unexposed hemoglobin. We conducted all other experiments at 37 °C where there is no aggregation, to avoid any possible interference of sample turbidity with spectrophotometrically measurements.

4. Conclusions

Our in vitro experiments led us to the following conclusions. The mobile phone frequencies of 910 and 940 MHz affect the O_2-binding ability of HbA (we have shown the data and figures relative to 940 MHz as a typical). The data relative to 910 MHz is resembled to 940 MHz (data not shown). In fact, Hb of a healthy human exposed to these frequencies bind less O_2 in the lung and releases more O_2 in the tissue. This change in the functional activity of HbA is due to changes in the tertiary structure of the protein at 37 °C. The alteration of structure of exposed HbA is accordance with diminishing and late aggregation process relative to unexposed sample.

Acknowledgements

The financial supports from the Research Council of the University of Tehran and Iran National Science Foundation (INSF) were acknowledged.

References

[1] E. Bismuto, F. Mancinelli, G. d'Ambrosio, R. Massa, Eur. Biophys. J. 32 (2003) 628–634.
[2] J.A. Laurence, P.W. French, R.A. Lindner, D.R. McKenzie, J. Theor. Biol. 206 (2000) 291–298.
[3] J.A. Laurence, D.R. McKenzie, K.R. Foster, J. Theor. Biol. 222 (2003) 403–405.
[4] H. Bohr, J. Bohr, Bioelectromagnetics 2 (2000) 68–72.
[5] H. Bohr, J. Bohr, Phys. Rev. E61 (2000) 4310–4314.
[6] R.D. Astumian, Phys. Rev. Lett. 91 (2003) 1181021–1181024.
[7] D.I. de Pomerai, B. Smith, A. Dawe, K. North, T. Smith, D.B. Archer, I.R. Duce, D. Jones, E.P. Candido, FEBS Lett. 543 (2003) 93–97.
[8] A.B. Copty, Y. Neve-Oz, I. Barak, M. Golosovsky, D. Davidov, Biophys. J. 91 (2006) 1413–1423.
[9] M. Blank, Electromagn. Biol. Med. 27 (2008) 3–23.
[10] D.F. George, M.M. Bilek, D.R. McKenzie, Bioelectromagnetics 29 (2008) 324–330.
[11] F. Mancinelli, M. Caraglia, A. Abbruzzese, G. d'Ambrosio, R. Massa, E. Bismuto, J. Cell. Biochem. 93 (2004) 188–196.
[12] T.Y. Zhao, S.P. Zou, P.E. Knapp, Neurosci. Lett. 412 (2007) 34–38.
[13] R. Nylund, D. Leszczynski, Proteomics 6 (2006) 4769–4780.
[14] M. Lantow, M. Lupke, J. Frahm, M.O. Mattsson, N. Kuster, M. Simko, Radiat. Environ. Biophys. 45 (2006) 55–62.
[15] M. Simkó, C. Hartwig, M. Lantow, M. Lupke, M.O. Mattsson, Q. Rahman, J. Rollwitz, Toxicol. Lett. 161 (2006) 73–82.
[16] J.W. Finnie, Pathology 37 (2005) 231–233.
[17] S. Lange, T. Viergutz, M. Simkó, Cell Prolif. 37 (2004) 337–349.
[18] J. Czyz, K. Guan, Q. Zeng, T. Nikolova, A. Meister, F. Schönborn, J. Schuderer, N. Kuster, A.M. Wobus, Bioelectromagnetics 25 (2004) 296–307.
[19] K. Yao, K.J. Wang, Z.H. Sun, J. Tan, W. Xu, L.J. Zhu, D.Q. Lu, Mol. Vis. 10 (2004) 138–143.
[20] J. Friedman, S. Kraus, Y. Hauptman, Y. Schiff, R. Seger, Biochem. J. 405 (2007) 559–568.
[21] K. Zwirska-Korczala, J. Jochem, M. Adamczyk-Sowa, P. Sowa, R. Polaniak, E. Birkner, M. Latocha, K. Pilc, R. Suchanek, J. Physiol. Pharmacol. 56 (2005) 101–108.
[22] S. Zhu, Y. Wu, Z. Yu, X. Zhang, H. Li, M. Gao, Bioresour. Technol. 97 (2006) 1964–1968.
[23] M. Blank, Bioelectromagnetics 26 (2005) 677–683.
[24] T. Vukova, A. Atanassov, R. Ivanov, N. Radicheva, Med. Sci. Monit. 11 (2005) BR50–BR56.
[25] M. Barteria, A. Palab, S. Rotellaa, Biophys. Chem. 113 (2005) 245–253.
[26] M. Portaccio, P. De Luca, D. Durante, S. Rossi, U. Bencivenga, P. Canciglia, M. Lepore, A. Mattei, A. De Maio, D.G. Mita, Bioelectromagnetics 24 (2003) 449–456.
[27] M. Ammari, A. Lecomte, M. Sakly, H. Abdelmelek, R. de-Seze, Toxicology 250 (2008) 70–74.
[28] A. Schirmacher, S. Winters, S. Fischer, J. Goeke, H.J. Galla, U. Kullnick, E.B. Ringelstein, F. Stögbauer, Bioelectromagnetics 21 (2000) 338–345.
[29] M. Blank, R. Goodman, Bioelectromagnetics 18 (1997) 111–115.
[30] H. Lin, L. Han, M. Blank, M. Head, R. Goodman, J. Cell. Biochem. 70 (1998) 297–303.
[31] M. Blank, R. Goodman, J. Cell. Biochem. 73 (1999) 369–374.
[32] M. Blank, R. Goodman, J. Cell. Biochem. 81 (2001) 689–692.
[33] M. Blank, L. Soo, Bioelectrochemistry 53 (2001) 171–174.
[34] M. Blank, L. Soo, J. Cell. Biochem. 81 (2001) 278–283.
[35] R. Goodman, M. Blank, J. Cell. Physiol. 192 (2002) 16–22.
[36] M. Blank, L. Soo, Bioelectrochemistry 61 (2003) 93–97.
[37] M. Blank, R. Goodman, J. Cell. Physiol. 199 (2004) 359–363.
[38] M. Blank, R. Goodman, J. Cell. Physiol. 214 (2008) 20–26.
[39] M. Blank, L. Soo, Bioelectrochem. Bioenerg. 45 (1998) 253–259.
[40] C. Schwarz, E. Kratochvil, A. Pilger, N. Kuster, F. Adlkofer, H.W. Rüdiger, Int. Arch. Occup. Environ. Health 81 (2008) 755–767.
[41] C.F. Martino, D. Belchenko, V. Ferguson, S. Nielsen-Preiss, H.J. Qi, Bioelectromagnetics 29 (2008) 125–132.
[42] S. Dasdag, M.Z. Akdag, E. Ulukaya, A.K. Uzunlar, D. Yegin, Arch. Med. Res. 39 (2008) 40–44.
[43] G. Stefanics, L. Kellényi, F. Molnár, G. Kubinyi, G. Thuróczy, I. Hernádi, BMC Public Health 12 (2007) 325–1325.
[44] N.E. Leadbeater, L.M. Stencel, E.C. Wood, Org. Biomol. Chem. 7 (2007) 1052–1055.
[45] H. Hirose, N. Sakuma, N. Kaji, K. Nakayama, K. Inoue, M. Sekijima, T. Nojima, J. Miyakoshi, Bioelectromagnetics 28 (2007) 99–108.

[46] A.R. Ferreira, F. Bonatto, M.A. de Bittencourt Pasquali, M. Polydoro, F. Dal-Pizzol, C. Fernández, A.A. de Salles, J.C. Moreira, Bioelectromagnetics 27 (2006) 487–493.
[47] Q. Zeng, G. Chen, Y. Weng, L. Wang, H. Chiang, D. Lu, Z. Xu, Proteomics 6 (2006) 4732–4738.
[48] T. Thorlin, J.M. Rouquette, Y. Hamnerius, E. Hansson, M. Persson, U. Björklund, L. Rosengren, L. Rönnbäck, M. Persson, Radiat. Res. 166 (2006) 409–421.
[49] J.R. Li, C.K. Chou, J.A. McDougall, G. Dasgupta, H.H. Wu, R.L. Ren, A. Lee, J. Han, J. Mom, Radiat. Res. 151 (1999) 710–716.
[50] J.A. Lukin, C. Ho, Chem. Rev. 104 (2004) 1219–1230.
[51] R.E. Dickerson, I. Geis, Hemoglobin: Structure, Function, Evolution, Pathology, Benjamin/Cummings Pub. Co. Inc, Redwood City, USA, 1983.
[52] E. Bennett-Guerrero, T.H. Veldman, A. Doctor, M.J. Telen, T.L. Ortel, T.S. Reid, M.A. Mulherin, H. Zhu, R.D. Buck, R.M. Califf, T.J. McMahon, Proc. Natl. Acad. Sci. U. S. A. 104 (2007) 17063–17068.
[53] S. Pin, C.A. Royer, E. Gratton, B. Alpert, G. Weber, Biochemistry 29 (1990) 9194–9202.
[54] N. Ramadas, J.M. Rifkind, Biophys. J. 76 (1999) 1796–1811.
[55] D.L. Nelson, M.M. Cox, Lehninger Principles of Biochemistry, Worth Publisher, New York, USA, 2005.
[56] M. Blank, J. Theor. Biol. 51 (1975) 127–134.
[57] G. di Prisco, S.G. Condo, M. Tamburrlnl, B. Giardlna, Trends Biochem. Sci. 16 (1991) 471–474.
[58] Y. Takashi, P. SungIck, T. Antonio, I. Kiyohiro, K. Kenji, J. Biol. Chem. 277 (2002) 34508–34520.
[59] E.M. Castilho, M.L. Glass, J.C. Manço, Braz. J. Med. Biol. Res. 36 (2003) 731–737.
[60] A. Rossi-Fanelli, E. Antonini, A. Caputo, J. Biol. Chem. 236 (1961) 391–396.
[61] R.E. Benesch, R. Benesch, C.I. Yu, Biochemistry 8 (1969) 2567–2571.
[62] E. Antonini, M. Brunori, Annu. Rev. Biochem. 39 (1970) 977–1042.
[63] N.W. Tietz, Textbook of Clinical Chemistry, W.B. Saunders Co, Philadelphia, USA, 1986.
[64] N. Rezaei-Ghaleh, H. Ramshini, A. Ebrahim-Habibi, A.A. Moosavi-Movahedi, M. Nemat-Gorgani, Biophys. Chem. 132 (2008) 23–32.
[65] S. Benjwal, S. Verma, K.H. Röhm, O. Gursky, Protein Sci. 15 (2006) 635–639.
[66] A. Barzegar, A.A. Moosavi-Movahedi, S. Rezaei-Zarchi, A.A. Saboury, M.R. Ganjali, P. Norouzi, G.H. Hakimelahi, F.Y. Tsai, Biotechnol. Appl. Biochem. 49 (2008) 203–211.
[67] T. Shirasawa, M. Izumizaki, Y. Suzuki, A. Ishihara, T. Shimizu, M. Tamaki, F. Huang, K. Koizumi, M. Iwase, H. Sakai, E. Tsuchida, K. Ueshima, H. Inoue, H. Koseki, T. Senda, T. Kuriyama, I. Homma, J. Biol. Chem. 278 (2003) 5035–5043.
[68] J.M. Salhany, Biochemistry 47 (2008) 6059–6072.
[69] T.R. Weiland, S. Kundu, J.T. Trent III, J.A. Hoy, M.S. Hargrove, J. Am. Chem. Soc. 126 (2004) 11930–11935.
[70] B.C. Vu, A.D. Jones, J.T. Lecomte, J. Am. Chem. Soc. 124 (2002) 8544–8545.
[71] B. Widdop, Ann. Clin. Biochem. 39 (2002) 378–391.
[72] L. Kiger, C. Poyart, M.C. Marden, Biochemistry 37 (1998) 14643–14650.
[73] S.L. Archer, V. Hampl, D.P. Nelson, E. Sidney, D.A. Peterson, E.K. Weir, Circ. Res. 77 (1995) 174–181.
[74] E.J. van Kampen, W.G. Zijlstra, Adv. Clin. Chem. 8 (1965) 141–185.
[75] M. Tkalec, K. Malaric, B. Pevalek-Kozlina, Bioelectromagnetics 26 (2005) 185–193.
[76] L.J. Challis, Bioelectromagnetics Supplement 7 (2005) S98–S106.
[77] A.A. Marinot, C. Frilot, Bioelectromagnetics 24 (2003) 70–72.
[78] R.K. Adair, Bioelectromagnetics 24 (2003) 440–441.
[79] Q. Balzano, Bioelectromagnetics 23 (2002) 278–287.
[80] Q. Balzano, Bioelectromagnetics 24 (2003) 483–488.
[81] Q. Balzano, A. Shepherd, Bioelectromagnetics 24 (2003) 473–482.
[82] Y. Sugita, I. Nagai, Y. Yoneyama, J. Biol. Chem. 246 (1971) 383–388.
[83] C. Liu, A. Bo, G. Cheng, X. Lin, S. Dong, Biochim. Biophys. Acta 1385 (1998) 53–60.
[84] H. Hamaguchi, A. Isomoto, H. Nakajima, Biochem. Biophys. Res. Commun. 35 (1969) 6–11.
[85] S. De, A. Girigoswami, J. Colloid. Interf. Sci. 296 (2006) 324–331.
[86] K.W. Olsen, Methods Enzymol. 231 (1994) 514–524.